KKU SCIENCE JOURNAL
Journal Home Page : https://ph01.tci-thaijo.org/index.php/KKUSciJ
Published by the Faculty of Science, Khon Kaen University, Thailand

แบบจำลองรังสีอัลตราไวโอเลตที่มีผลต่อผิวหนังมนุษย์ในประเทศไทยโดยใช้โครงข่ายประสาทเทียมและ Extreme Gradient Boosting

Modeling Erythemal Ultraviolet Radiation in Thailand using Artificial Neural Networks (ANN) and Extreme Gradient Boosting (XGBoost)

ชนินาถ ศรีเมือง[1] สุมามาลย์ บรรเทิง[1*] สมเจตน์ ภัทรพานิชชัย[1] จรุงแสง ลักษณบุญส่ง[1] และ เสริม จันทร์ฉาย[1]

Chaninat Srimueang[1], Sumaman Buntoung[1*], Somjet Pattarapanitchai[1], Jarungsang Laksanaboonsong[1] and Serm Janjai[1]

[1]ภาควิชาฟิสิกส์ คณะวิทยาศาสตร์ มหาวิทยาลัยศิลปากร วิทยาเขตพระราชวังสนามจันทร์ จังหวัดนครปฐม 73000

[1]Department of Physics, Faculty of Science, Silpakorn University, Sanam Chandra Palace Campus, Muang, Nakhon Pathom 73000, Thailand

บทคัดย่อ

งานวิจัยนี้มีวัตถุประสงค์ในการประมาณค่ารังสีอัลตราไวโอเลตที่มีผลต่อผิวหนังมนุษย์ภายใต้ทุกสภาพท้องฟ้าด้วยตัวแปรทางบรรยากาศและอุตุนิยมวิทยาโดยใช้แบบจำลองการเรียนรู้ของเครื่อง ข้อมูลที่ใช้ในงานวิจัยรวบรวมมา ณ ตำแหน่งสถานีวัดภาคพื้นดิน 4 แห่ง ในภูมิภาคต่าง ๆ ของประเทศไทย ได้แก่ เชียงใหม่ อุบลราชธานี สงขลา และนครปฐม ตั้งแต่ปี ค.ศ. 2019 ถึง ค.ศ. 2023 ในงานวิจัยนี้ใช้แบบจำลองการเรียนรู้ของเครื่อง 2 แบบจำลอง ได้แก่ โครงข่ายประสาทเทียมและ XGBoost และทำการเปรียบเทียบประสิทธิภาพของแบบจำลองทั้งสอง ผลการวิจัยที่ได้พบว่าแบบจำลอง XGBoost สามารถประมาณค่ารังสีอัลตราไวโอเลตที่มีผลต่อผิวหนังมนุษย์ได้แม่นยำกว่าแบบจำลองโครงข่ายประสาทเทียม โดยให้ค่านอร์มัลไลซ์ของรากที่สองของค่าความคลาดเคลื่อนเฉลี่ยกำลังสองอยู่ในช่วง 8.56% ถึง 14.32% แสดงให้เห็นว่าแบบจำลอง XGBoost มีประสิทธิภาพในการประมาณค่ารังสีอัลตราไวโอเลตในประเทศไทยได้ดีและสามารถนำไปต่อยอดพัฒนาการพยากรณ์รังสีอัลตราไวโอเลตที่มีผลต่อผิวหนังมนุษย์ได้ต่อไป

ABSTRACT

This study proposes machine learning models to estimate erythemal ultraviolet (EUV) radiation under all sky conditions using several available atmospheric and meteorological parameters. Data at four ground-based stations in key regions of Thailand namely, Chiang Mai, Ubon Ratchathani, Songkhla, and Nakhon Pathom, were collected from 2019 to 2023. Two well-known machine learning techniques, Artificial Neural Networks (ANN) and Extreme Gradient Boosting (XGBoost), were developed and employed, and their

*Corresponding Author, E-mail: Buntoung_s@silpakorn.edu

Received date: 25 April 2025| Revised date: 8 August 2025 | Accepted date: 13 August 2025
doi: 10.14456/kkuscij.2025.34

performance was compared. The results show that XGBoost outperformed ANN in terms of accuracy, with the best performance at each site yielding normalized root mean square errors (nRMSE) ranging from 8.56% to 14.32%. This superior performance suggests that XGBoost is more effective for estimating EUV radiation in Thailand and could be further improved for radiation forecasting.

คำสำคัญ: รังสีอัลตราไวโอเลตที่มีผลต่อผิวหนังมนุษย์ การเรียนรู้ของเครื่อง เอ็กซ์จีบูสต์ โครงข่ายประสาทเทียม
Keywords: Erythemal Ultraviolet Radiation, Machine Learning, XGBoost, ANN

INTRODUCTION

Ultraviolet (UV) radiation is a component of solar radiation and can be categorized into three types based on their wavelength ranges. Ultraviolet C (UV-C) has a wavelength range of 100 - 280 nm, ultraviolet B (UV-B) ranges from 280 - 315 nm, and ultraviolet A (UV-A) spans from 315 - 400 nm (WHO 2002). The amount of UV radiation reaching the Earth's surface is influenced by various factors, including atmospheric components such as ozone, aerosols, clouds, and water vapor. Additionally, the geometry of a location on the Earth relative to the sun such as the distance between the Earth and the sun, the solar zenith angle, and the Earth's axial tilt also affects the intensity of UV radiation (Prasad *et al*., 2023).

The ultraviolet radiation that reaches the Earth's surface, specifically UV-A and UV-B, accounts for only 5 - 7% of the total solar radiation (Roshan *et al*., 2020; Ahmed *et al*., 2022). Nevertheless, it is considered an important type of radiation for human health, the environment, and ecosystems (Rivas *et al*., 2020). Regarding human health, particularly the skin, exposure to UV radiation can have both positive and negative effects. On the positive side, UV radiation helps synthesize vitamin D, which strengthens bones and supports a healthy immune system (Juzeniene and Moan, 2012; Webb *et al*., 2021). In medicine, it is also used to treat conditions such as atopic dermatitis, psoriasis, and vitiligo (Elmets *et al*., 2019). On the negative side, overexposure can lead to premature wrinkles, freckles, or even skin cancer (Bilbao *et al*., 2014). However, the occurrence of these effects depends on the amount of UV radiation received, as well as factors like age, gender, and skin color. The UV radiation associated with these effects is identified by the International Commission on Illumination (CIE) as erythemal UV (EUV) radiation (CIE, 2006), which causes redness in the human skin. This weighted UV radiation can be converted into UV index, which is more commonly promoted in society (WHO, 2002).

Generally, the amount of UV radiation at the Earth's surface can be obtained directly from ground-based measurements. However, due to high costs and maintenance requirements, the installation of such instruments is very limited. Therefore, modeling is an alternative option to estimate UV radiation. There are several approaches to estimate UV radiation, such as empirical models and physical models (Antón *et al*., 2009; Janjai *et al*., 2010a). Recently, Artificial Intelligence (AI) approaches, such as machine learning models, have become increasingly popular and offer high performance. These models effectively capture nonlinear relationships and learn temporal patterns in input and output variables, making them well-suited for predicting solar radiation influenced by rapidly changing weather conditions such as clouds and aerosols, which are difficult to model with conventional methods (Prasad *et al*., 2023). Consequently, several recent

studies have applied machine learning models to estimate or forecast solar radiation including UV radiation in different regions around the world such as Australia (Prasad *et al*., 2025; Ahmed *et al.*, 2022), Thailand (Raksasat *et al*., 2021), Spain (Dieste-Velasco *et al.*, 2023), and Turkey (Demir and Citakoglu, 2023). In case of UV radiation, Ahmed *et al.* (2022) forecasted the UV Index in Perth, Australia, using several hybrid deep learning models based on atmospheric and meteorological variables, as well as climate indices. Dieste-Velasco *et al.* (2023) explored the performance of Artificial Neural Networks (ANN) and regression models for estimating UV radiation (280 - 400 nm) in Burgos, Spain, using meteorological data. The results showed that ANN provided greater accuracy than the regression approaches.

In Thailand, studies on solar UV radiation have received limited attention (Janjai *et al.*, 2010b; Raksasat *et al.*, 2021; Laiwarin *et al.*, 2024), partly due to the high cost of measurement instruments and the need for regular maintenance to ensure data quality, despite the fact that UV radiation levels are notably high. Given the potential health risks associated with excessive UV exposure, it is crucial to improve our understanding and prediction of these radiation levels. Therefore, this study focuses on developing two well-known machine learning models, Extreme Gradient Boosting (XGBoost) and ANN, as they can effectively capture complex nonlinear relationships present in atmospheric variables. This makes them practical and efficient tools for estimating EUV radiation under all sky conditions in Thailand. Another aim is to use easily accessible and readily available input data.

MATERIALS AND METHODS

In this study, four different climate locations in Thailand are selected based on the availability of ground-based data. The first site is located in the northern part of Thailand, Chiang Mai (18.78°N, 98.98°E), in a meteorological center. The second site is in a meteorological center in Ubon Ratchathani (15.25°N, 104.87°E), the northeastern part of the country. The third site is located in the central region, at Silpakorn University, Nakhon Pathom (13.82°N, 100.04°E). Finally, the Songkhla site (7.20°N, 100.60°E), located at a meteorological center in the southeastern part of Thailand. The climate at these sites is influenced by two local monsoons: the northeast and southwest monsoons. These bring cool air masses during the winter season, warm and humid conditions during the summer, and heavy rainfall during the rainy season to the sites. However, Songkhla, which is located on the eastern coast and in the southern part of the country, has a distinctly different climate compared to the other stations due to its coastal location. The climate in Songkhla is characterized by high humidity and significant rainfall throughout the year, with no distinct dry season. The locations of these sites are shown in Figure 1.

At each site, a UV-Biometer (501A, Solar Light Company) was installed on the rooftop of the building (Figure 1), and voltage signals were recorded every second using a datalogger (DX2000, Yokogawa). The voltages were converted to EUV irradiance in watt per square meter (W/m^2) following the standard procedure described in Webb *et al*. (2006). This method was also used in the work of Janjai *et al.* (2010b). These data were quality controlled using the criteria outlined in Bilbao and de Migue (2020), which stated that EUV should not exceed 1.2 times the extraterrestrial EUV irradiance, as well as the procedure described

in Janjai *et al.* (2010b). Erroneous data were subsequently rejected. The EUV irradiances were then averaged over each hour, and these data were referred to as hourly EUV irradiance from 07:00 to 17:00 local time. In this study, the hourly EUV irradiance at 7:00, 10:00, 13:00, and 16:00 local time was used as the model output. Variations in EUV irradiance at the four sites, which change significantly with the seasons and are influenced by atmospheric components, have been reported in the work of Janjai *et al.* (2010a; 2010b).

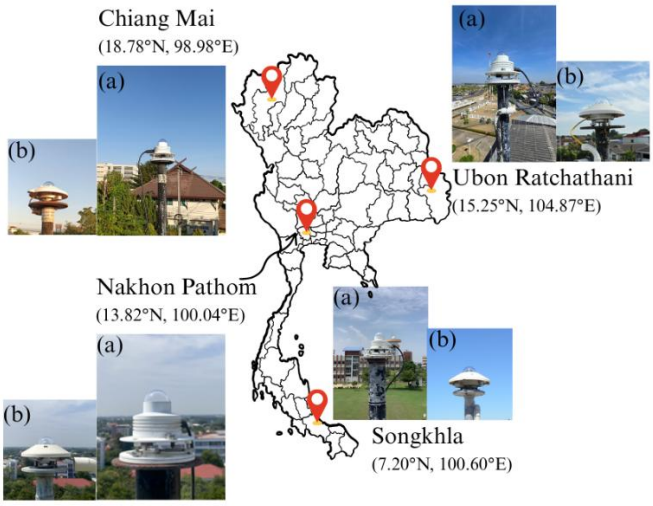

Figure 1 The locations of the studied sites in Thailand where (a) UV-Biometers and (b) pyranometers were installed.

For the input of the model, several atmospheric compositions and meteorological variables that affect the variations of EUV radiation were considered. These include global broadband irradiance (I_{GB}), extraterrestrial EUV irradiance (EUV_0), cloud cover (CC), visibility (VIS), total column ozone (O_3), and air temperature (T). These data are available and easily accessible within the country. Broadband irradiance was measured by a pyranometer (CM21, Kipp&Zonen) at each site, and data acquisition was the same as for the UV-Biometer. Cloud cover and visibility were observed by meteorological professionals at Chiang Mai, Ubon Ratchathani, Songkhla, and Nakhon Pathom (14.01°N, 99.97°E) meteorological stations, and provided on a three-hourly basis at 7:00, 10:00, 13:00, and 16:00 local time. Air temperature data were retrieved from the National Center for Environmental Prediction (NCEP) and The National Center for Atmospheric Research (NCAR) (Kalnay *et al*., 1996). The data were provided on a six-hourly basis at 1:00, 7:00, 13:00, 19:00 local time. For total column ozone, the data were provided by National Aeronautics and Space Administration (NASA), measured by the Ozone Monitoring Instrument (OMI) on the AURA satellite. The data are available on a daily basis (Levelt *et al*., 2006).

Due to the different time resolutions of the datasets, and to minimize errors caused by excessive interpolation, we decided to estimate EUV irradiance at a 3-hour resolution. The total column ozone from OMI/AURA was set as constant throughout the day based on the fact that total column ozone typically does not vary significantly within a single day. Therefore, only the NCEP/NCAR data were interpolated using linear interpolation, due to its simplicity and effectiveness. Consequently, the prediction times were set at

07:00, 10:00, 13:00, and 16:00 local time to align with data availability and adequately capture daytime EUV variations. The information for all data used in this study is summarized in Table 1.

Table 1 The information of input and output of the models

Attribute name	Acronym	Source	Instrument	Unit
Erythemal ultraviolet irradiance	EUV	Ground	UV-Biometer	mW/m^2
Global broadband irradiance	I_{GB}	Ground	Pyranometer	W/m^2
Extraterrestrial erythemal ultraviolet irradiance	EUV_0	Calculation	Janjai *et al*. (2010a)	W/m^2
Cloud cover	CC	Ground	Observation	tenths
Visibility	VIS	Ground	Observation	km
Total column ozone	O_3	Satellite	OMI/AURA	DU
Air temperature	T	Reanalysis	NCEP/NCAR	ºC

ANN is a computational model that works like the human brain, consisting of layers of interconnected neurons that learn nonlinear relationships through training. It is widely used for its strong self-learning capabilities and high predictive accuracy (Dieste-Velasco *et al.*, 2023). Similarly, XGBoost is an efficient approach to gradient boosting that builds an ensemble of decision trees to correct errors sequentially. Moreover, due to its speed, accuracy, and robustness, XGBoost performs well on capturing complex patterns in data and is commonly applied in predictive tasks such as solar radiation forecasting (Prasad *et al.*, 2025).

In the modeling process, the input data presented in Table 1, covering the years 2019 to 2023, were used. Pearson correlation coefficients were calculated to assess the relationship between each input variable and EUV irradiance. The results showed that only global broadband irradiance and extraterrestrial EUV irradiance exhibited strong correlations ($r = 0.82 - 0.89$), while the remaining variables had relatively low coefficients ($r < 0.42$). Nevertheless, all six input parameters were retained in the model, as they are known to influence the attenuation and variability of UV radiation at the surface. Including these variables allows for a more comprehensive representation of the atmospheric conditions that affect EUV levels.

These data were randomly divided into three groups: training, validation, and testing datasets, using a ratio of 70:15:15. This ratio is not strictly fixed and may vary depending on the user's preference; however, a larger proportion is typically allocated to the training set. For example, the ratio of 68:12:20 used in Prasad *et al.* (2023), and Dieste-Velasco *et al.* (2023) employed in 70:15:15. Once the data were separated, each group was kept fixed and ensured to cover the full range of EUV values, from low to high. Additionally, the data selected in this work cover all sky conditions: clear, intermediate, and overcast, as verified using cloud cover data from Thai Meteorological Department (TMD). This ensures that the model is trained and tested under various atmospheric conditions, supporting its ability to generalize well. To incorporate temporal dependencies, time-lagged and previous-day data were included as inputs, allowing the model to learn from historical patterns and improve estimation accuracy.

The performance of the constructed model was tested with statistical matrics, including coefficient of determination (R^2), index of agreement (IOA), normalized mean bias error (nMBE), and normalized root mean square error (nRMSE) (Dieste-Velasco *et al.*, 2023). The equations can be represented as follows.

$$R^2 = 1 - \frac{\sum_{i=1}^{n}(EUV_{measured,i} - EUV_{model,i})^2}{\sum_{i=1}^{n}(EUV_{measured,i} - \overline{EUV}_{measured})^2} \quad (1)$$

$$IOA = 1 - \frac{\sum_{i=1}^{n}(EUV_{model,i} - EUV_{measured,i})^2}{\sum_{i=1}^{n}(|EUV_{model,i} - \overline{EUV}_{measured}| + |EUV_{measured,i} - \overline{EUV}_{measured}|)^2} \quad (2)$$

$$nMBE = \frac{\frac{1}{n}\sum_{i=1}^{n}(EUV_{model,i} - EUV_{measured,i})}{\overline{EUV}_{measured}} \times 100\% \quad (3)$$

$$nRMSE = \frac{\sqrt{\frac{1}{n}\sum_{i=1}^{n}(E_{model,i} - E_{measured,i})^2}}{\overline{EUV}_{measured}} \times 100\% \quad (4)$$

where $EUV_{measured}$ and EUV_{model} are the erythemal ultraviolet irradiance from the measurement and the model in mW/m^2, n is the number of data. $\overline{EUV}_{measured}$ is the averaged value of the erythemal ultraviolet irradiance from the measurement.

The R^2 indicates the proportion of variance in the measured data explained by the model; higher values denote better performance. The IOA, ranging from 0 to 1, assesses the degree of match between estimated and measured values, with values closer to 1 indicating stronger agreement. The nMBE reflects systematic bias in the estimation; values closer to zero suggest less bias. The nRMSE measures the average magnitude of errors; lower values indicate higher accuracy.

RESULTS AND DISCUSSION

Using all six input parameters, XGBoost and ANN were utilized in this study to estimate EUV irradiance in Thailand. Several trials were undertaken throughout the creation of the models. For the ANN, several hyperparameters were varied to achieve the best estimation performance, including the number of hidden layers (3), number of neurons (16, 32, 64, 128, 256), learning rate (0.01, 0.001, 0.0001), dropout rate (0.1, 0.2, 0.3), activation function (ReLU), number of epochs (200, 500, 1000), and batch size (64). Similarly, for the XGBoost model, the following hyperparameters were tuned: max depth (3, 5, 7), learning rate (0.01, 0.05, 0.10), number of estimators (200, 500, 800), subsample ratio (0.7, 0.8, 1.0), column sampling ratio by tree (colsample_bytree, 0.8), and random state (42). Grid search was applied for hyperparameter tuning to identify the optimal combination that yielded the best estimation performance. The selected parameters for each site are summarized in Table 2.

Table 2 Hyperparameters that yielded the best performance

Model	Parameter	Chiang Mai	Ubon Ratchathani	Nakhon Pathom	Songkhla
ANN	Hidden layer	3	3	3	3
	Neurons	256, 128, 64	128, 64, 32	128, 64, 32	256, 128, 64
	Learning rate	0.0001	0.0001	0.001	0.01
	Dropout rate	0.1	0.1	0.2	0.2
	Activation function	ReLU	ReLU	ReLU	ReLU
	Epoch	1000	500	500	1000
	Batch size	64	64	64	64
XGBoost	Max depth	5	5	5	5
	N_estimators	0.05	0.05	0.1	0.1
	Subsample	800	800	500	800
	Colsample_bytree	0.8	0.7	0.8	0.8
	Learning rate	0.8	0.8	0.8	0.8
	Random state	42	42	42	42

Using the parameters in Table 2, the best performances for estimating the radiation are shown in Table 3. It is clear that the performance of XGBoost is better than ANN for all sites. The comparison between the EUV irradiance from the measurement and the XGBoost model are presented as scatter plots in Figure 2.

Table 3 Comparison of the performance of ANN and XGBoost models

Site name	ANN				XGBoost			
	R^2	IOA	nMBE (%)	nRMSE (%)	R^2	IOA	nMBE (%)	nRMSE (%)
Chiang Mai	0.98	0.99	0.75	10.91	0.98	1.00	0.55	10.47
Ubon Ratchathani	0.94	0.99	1.90	16.06	0.96	0.99	1.84	14.30
Nakhon Pathom	0.95	0.99	- 0.89	14.60	0.96	0.99	- 1.43	14.32
Songkhla	0.99	1.00	0.81	9.65	0.99	1.00	0.28	8.56

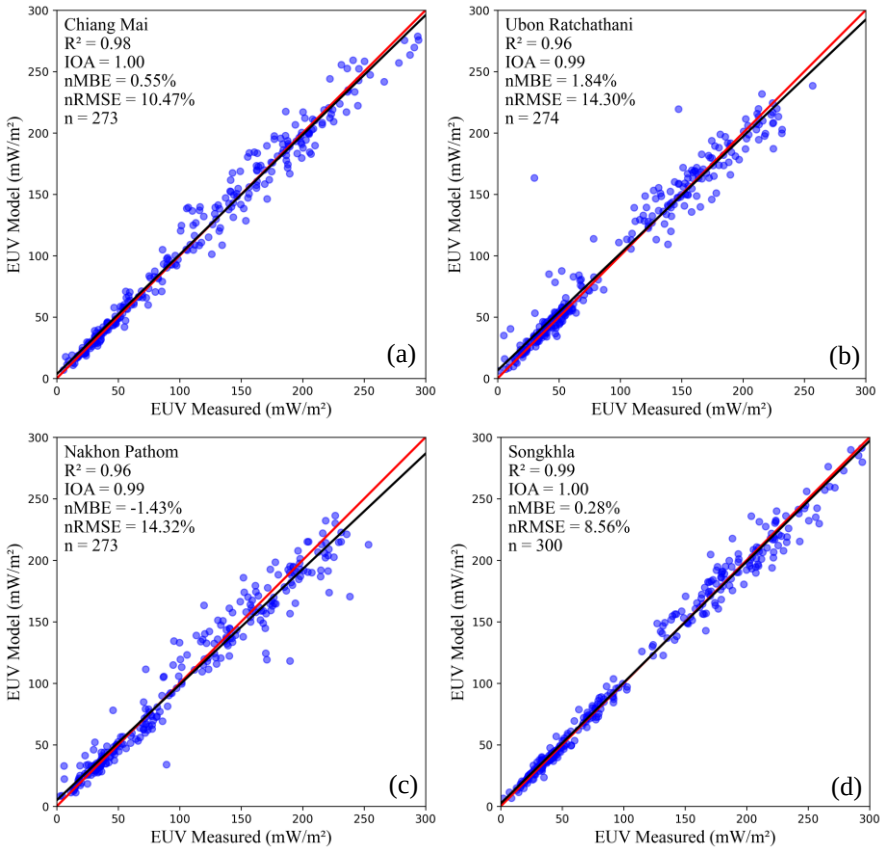

Figure 2 Scatter plots comparing the measured erythemal ultraviolet irradiance (EUV Measured) with predictions from the XGBoost model (EUV Model) at Chiang Mai (a), Ubon Ratchathani (b), Nakhon Pathom (c), and Songkhla (d). The red line represents the 1:1 line, the black line represents the regression line, and n denotes the number of data points.

Therefore, XGBoost was chosen to optimize the number of input variables, using the same model configuration and testing dataset as in Table 3. In this analysis, input variables were removed one at a time, and the model's performance was compared. However, global broadband irradiance and extraterrestrial EUV irradiance were retained in all trials, as they showed high Pearson correlation coefficients with EUV irradiance. The performance results are shown in Table 4.

Table 4 Comparison of the model performance when reducing the number of inputs

Site name	Input variable	XGBoost			
		R^2	IOA	nMBE (%)	nRMSE (%)
Chiang Mai	I_{GB}, EUV_0, CC, O_3, VIS, T	0.98	1.00	0.55	10.47
	I_{GB}, EUV_0, CC, O_3, VIS	0.98	0.99	0.90	10.81
	I_{GB}, EUV_0, CC, O_3, T	0.98	0.99	0.54	10.93
	I_{GB}, EUV_0, CC, VIS, T	0.98	0.99	0.62	10.96
	I_{GB}, EUV_0, O_3, VIS, T	0.98	0.99	- 0.02	10.74
Ubon Ratchathani	I_{GB}, EUV_0, CC, O_3, VIS, T	0.96	0.99	1.83	14.30
	I_{GB}, EUV_0, CC, O_3, VIS	0.95	0.99	1.79	15.10
	I_{GB}, EUV_0, CC, O_3, T	0.95	0.99	1.91	14.63
	I_{GB}, EUV_0, CC, VIS, T	0.95	0.99	1.95	15.70
	I_{GB}, EUV_0, O_3, VIS, T	0.95	0.99	2.24	15.56
Nakhon Pathom	I_{GB}, EUV_0, CC, O_3, VIS, T	0.96	0.99	- 1.43	14.32
	I_{GB}, EUV_0, CC, O_3, VIS	0.95	0.99	- 0.90	14.73
	I_{GB}, EUV_0, CC, O_3, T	0.95	0.99	- 1.32	15.64
	I_{GB}, EUV_0, CC, VIS, T	0.94	0.98	- 0.72	16.81
	I_{GB}, I_{EUV0}, O_3, VIS, T	0.94	0.98	- 0.91	16.66
Songkhla	I_{GB}, EUV_0, CC, O_3, VIS, T	0.99	1.00	0.28	8.56
	I_{GB}, EUV_0, CC, O_3, VIS	0.99	1.00	0.34	8.95
	I_{GB}, EUV_0, CC, O_3, T	0.99	1.00	0.83	9.36
	I_{GB}, EUV_0, CC, VIS, T	0.98	1.00	- 0.10	10.05
	I_{GB}, EUV_0, O_3, VIS, T	0.99	1.00	0.39	8.93

From the results shown in Table 4, it could be seen that using different input combinations led to slight variations in nRMSE values. For example, at Nakhon Pathom station, when using all six parameters, the nRMSE was 14.32%, while excluding T resulted in an nRMSE of 14.73%. To determine whether these differences were statistically significant, an additional analysis was performed using the Friedman test, followed by the Wilcoxon signed-rank test (Rainio *et al*., 2024). However, since the Friedman test could not be applied directly to nRMSE values, in this study, the Friedman analysis was conducted based on mean absolute error (MAE). The results showed that excluding the O_3 variable at Ubon Ratchathani (p = 0.0019), Nakhon Pathom (p = 0.0015), and Songkhla (p = 0.0044) stations produced significantly different outcomes compared to using all input variables at the 95% confidence level. In contrast, for other variables and at Chiang Mai station, *p - values* were greater than 0.05, indicating no significant differences. These results indicated that, for the three stations, excluding O_3 led to an increase in nRMSE, suggesting that O_3 was an important input variable that contributed positively to the model's prediction accuracy. However, at Chiang Mai site, the model appeared less sensitive to the exclusion of individual input variables, which might have

reflected complex atmospheric influences in the region that diminished the apparent importance of any single variable. Based on these findings, we recommend using all six parameters, as it generally yields lower nRMSE, ranging from 8.56% to 14.32%, and ensures robust performance across different stations.

When comparing our results with previous studies, the nRMSE values obtained in this work range from 8.56% to 14.32%, which were comparable to those reported by Ahmed *et al.* (2022) (2% to 26%), García-Rodríguez *et al.* (2023) (12.35% to 19.20%) and Dieste-Velasco *et al.* (2023) (3.77% to 46.05%). Furthermore, when compared with a study in Thailand, the machine learning approaches used in this study appeared to provide better estimations of UV values than the empirical methods used by Laiwarin *et al.* (2024). This comparison demonstrated that the models proposed here achieve competitive performance in estimating EUV irradiance.

CONCLUSIONS

In conclusion, machine learning techniques, ANN and XGBoost, were successfully applied to estimate erythemal ultraviolet irradiance, a key factor affecting human health. The models utilized six input variables that account for the variation in erythemal ultraviolet radiation at the Earth's surface: global broadband irradiance, extraterrestrial erythemal UV irradiance, cloud cover, visibility, total column ozone, and air temperature. These variables are typically obtained from ground-based and reanalysis data measurements within the country. The XGBoost model outperformed the ANN model in terms of estimating radiation, and incorporating all six variables led to enhanced accuracy. This approach holds promise for future applications in forecasting erythemal ultraviolet radiation, helping to raise awareness and protect human health from harmful sun exposure.

ACKNOWLEDGEMENTS

This research is financially supported by the Thailand Science Research and Innovation (TSRI) National Science, Research, and Innovation Fund (NSRF) for the Fiscal Year 2024. Srimueang, C. also received funding as a research assistant for her Master's degree from the Faculty of Science, Silpakorn University. The authors would like to express their gratitude to the Thai Meteorological Department for providing the data and assisting with the maintenance of our instruments at the research sites.

REFERENCES

Ahmed, A.A.M., Ahmed, M.H., Saha, S.K., Ahmed, O. and Sutradhar, A. (2022). Optimization algorithms as training approach with hybrid deep learning methods to develop an ultraviolet index forecasting model. Stochastic Environmental Research and Risk Assessment 36: 3011 - 3039. doi: 10.1007/s00477-022-02177-3.

Antón, M., Serrano, A., Cancillo, M.L. and García, J.A. (2009). An empirical model to estimate ultraviolet erythemal transmissivity. Annales Geophysicae 27(4): 1387 - 1398. doi: 10.5194/angeo-27-1387-2009.

Bilbao, J. and de Migue, A. (2020). Erythemal Solar Irradiance, UVER, and UV Index from Ground-Based Data in Central Spain. Applied Sciences 10(18): 6589. doi: 10.3390/app10186589.

Bilbao, J., Román, R., Yousif, C., Mateos, D. and de Miguel, A. (2014). Total ozone column, water vapour and aerosol effects on erythemal and global solar irradiance in Marsaxlokk, Malta. Atmos Environ. 99: 508 - 518. doi: 10.1016/j.atmosenv.2014.10.005.

Commission Internationale de l'éclairage (2006). Action Spectrum for the Production of Previtamin D3 in Human Skin. CIE 174:2006. International Commission on Illumination.

Demir, V. and Citakoglu, H. (2023). Forecasting of solar radiation using different machine learning approaches. Neural Computing and Applications 35: 887 - 906. doi: 10.1007/s00521-022-07841-x.

Dieste-Velasco, M.I., García-Rodríguez, S., García-Rodríguez, A., Díez-Mediavilla, M. and Alonso-Tristán, C. (2023). Modeling horizontal ultraviolet irradiance for all sky conditions by using Artificial Neural Networks and regression models. Applied Sciences 13(3): 1473. doi: 10.3390/app13031473.

Elmets, C.A., Lim, H.W., Stoff, B., Connor, C., Cordoro, K.M., Lebwohl, M., Armstrong, A.W., Davis, D.M.R., Elewski, B.E., Gelfand, J.M., Gordon, K.B., Gottlieb, A.B., Kaplan, D.H., Kavanaugh, A., Kiselica, M., Kivelevitch, D., Korman, N.J., Kroshinsky, D., Leonardi, C.L., Lichten, J., Mehta, N.N., Paller, A.S., Parra, S.L., Pathy, A.L., Farley Prater, E.A., Rupani, R.N., Siegel, M., Strober, B.E., Wong, E.B., Wu, J.J., Hariharan, V. and Menter, A. (2019). Joint American Academy of Dermatology-National Psoriasis Foundation guidelines of care for the management of psoriasis with phototherapy. Journal of the American Academy of Dermatology 81(3): 775 - 804. doi: 10.1016/j.jaad.2019.11.024.

García-Rodríguez, S., García-Rodríguez, A., Granados-López, D., García, I. and Alonso-Tristán, C. (2023). Ultraviolet erythemal irradiance (UVER) under different sky conditions in Burgos, Spain: Multilinear regression and Artificial Neural Network models. Applied Sciences 13(19): 10979. doi: 10.3390/app 131910979.

Janjai, S., Buntoung, S., Wattan, R. and Masiri, I. (2010a). Mapping solar ultraviolet radiation from satellite data in a tropical environment. Remote Sensing of Environment 114(3): 682 - 691. doi: 10.1016/j.rs e.2009.11.008.

Janjai, S., Kirdsiri, K., Masiri, I. and Nunez, M. (2010b). An investigation of solar erythemal ultraviolet radiation in the tropics: a case study at four stations in Thailand. International Journal of Climatology 30: 1893 - 1903. doi: 10.1002/joc.2006.

Juzeniene, A. and Moan, J. (2012). Beneficial effects of UV radiation other than via vitamin D production. Dermato-Endocrinology 4(2): 109 - 117. doi: 10.4161/derm.20013.

Kalnay, E., Kanamitsu, M., Kistler, R., Collins, W., Deaven, D., Gandin, L., Iredell, M., Saha, S., White, G., Woollen, J., Zhu, Y., Chelliah, M., Ebisuzaki, W., Higgins, W., Janowiak, J., Mo, K.C., Ropelewski, C., Wang, J., Leetmaa, A., Reynolds, R., Jenne, R. and Joseph, D. (1996). The NCEP/NCAR 40-year reanalysis project. Bulletin of the American Meteorological Society 77(3): 437 - 472.

Laiwarin, P., Buntoung, S. and Janjai, S. (2024). Development of empirical models for calculating global and diffuse erythemal weighted solar ultraviolet radiation under clear sky conditions in Thailand. Science, Engineering and Health Studies 18: 24020003.

Levelt, P.F., van den Oord, G.H.J., Dobber, M.R., Malkki, A., Visser, H., de Vries, J., Stammes, P., Lundell, J.O.V. and Saari, H. (2006). The ozone monitoring instrument. IEEE Transactions on Geoscience and Remote Sensing 44(5): 1093 - 1101. doi: 10.1109/TGRS.2006.872333.

Prasad, S.S., Deo, R.C., Salcedo-Sanz, S., Downs, N.J., Casillas-Pérez, D. and Parisi, A.V. (2023). Enhanced joint hybrid deep neural network explainable artificial intelligence model for 1-hr ahead solar ultraviolet index prediction. Computer Methods and Programs in Biomedicine 241: 107737. doi: 10.1016 /j.cmpb.2023.107737.

Prasad, S.S., Joseph, L.P., Ghimire, S., Deo, R.C., Downs, N.J., Acharya, R. and Yaseen, Z.M. (2025). Explainable hybrid deep learning framework for enhancing multi-step solar ultraviolet-B radiation predictions. Atmospheric Environment 343: 120951. doi: 10.1016/j.atmosenv.2024.120951.

Rainio, O., Teuho, J. and Klén, R. (2024). Evaluation metrics and statistical tests for machine learning. Scientific Reports 14: 6086. doi: 10.1038/s41598-024-56706-x.

Raksasat, R., Sri-iesaranusorn, P., Pemcharoen, Laiwarin, P., Buntoung, S., Janjai, S., Boontaveeyuwat, E., Asawanonda, P., Sriswasdi, S. and Chuangsuwanich, E. (2021). Accurate surface ultraviolet radiation forecasting for clinical applications with deep neural network. Scientific Reports 11: 5031. doi: 10.10 38/s41598-021-84396-2.

Rivas, M., Calaf, G.M., Laroze, D., Rojas, E., Mendez, J., Honeyman, J. and Araya, M.C. (2020). Solar ultraviolet A radiation and nonmelanoma skin cancer in Arica, Chile. Journal of Photochemistry and Photobiology B: Biology 212: 112047. doi: 10.1016/j.jphotobiol.2020.112047.

Roshan, D.R., Koç, M., Abdallah, A.A., Pomares, L.M., Isaifan, R. and Fountoukis, C. (2020). UV index forecasting under the influence of desert dust: Evaluation against surface and satellite-retrieved data. Atmosphere 11(1): 96.

Webb, A., Gröbner, J. and Blumthaler, M. (2006). COST-726: A practical guide to operating broadband instruments measuring erythemally weighted irradiance. EU Publications Office. No. EUR22595.

Webb, A.R., Alghamdi, R., Kift, R. and Rhodes, L.E. (2021). 100 YEARS OF VITAMIN D: Dose-response for change in 25-hydroxyvitamin D after UV exposure: outcome of a systematic review. Endocrine Connections 10(10): R248 - R266. doi: 10.1530/EC-21-0308.

WHO (2002). Global solar UV index: A practical guide (A joint recommendation of World Health Organization, World Meteorological Organization, United Nations Environment Programme, International Commission on Non-Ionizing Radiation Protection). Geneva: World Health Organization.

❑❑❑❑❑